Radio Wave Characterization and Modeling in Underground Mine Tunnels

Mathieu Boutin, Ahmed Benzakour, Charles L. Despins, *Senior Member, IEEE*, and Sofiène Affes, *Senior Member, IEEE*

***Abstract*—Results are presented on wideband radio propagation measurements and statistical modeling at 2.4 GHz and 5.8 GHz in real underground mine tunnels. This peculiar type of confined environment is characterized by very rough surfaces and a frequent absence of a line-of-sight between transmitting and receiving antennas. The resulting propagation characteristics differ from those frequently encountered in more typical indoor environments such as offices and corridors. Indeed, the rms delay spread shows little or no correlation with respect to transmitter-receiver distance and, in addition, no impulse response path arrival clustering effect is observed. However, the path amplitude distribution does tend to follow a Rice distribution in the line-of-sight case, and a Rayleigh distribution otherwise.**

***Index Terms*—Characterization, path amplitude, path arrival, propagation, radio wave, statistical modeling, tunnels, underground mine, wideband.**

I. Introduction

THIS paper describes the results of a measurement campaign performed at frequencies of 2.4 GHz and 5.8 GHz in a real underground mine. This former gold mine is located approximately 530 kilometers north-west of Montreal and is now managed by the Government of Canada as an experimental mine (named *CANMET*), in which *in-situ* tests and trials can be performed in a realistic environment. This type of confined environment differs significantly from conventional indoor environments (e.g., offices) as a result of narrow labyrinths with rough surfaces, curvatures, side galleries, etc. Wideband characterization of the underground channel is presented, with a particular focus on path loss effects and impulse response structure, followed by statistical modeling and simulation of the propagation channel, based on the appropriate models. As is noted in various parts of this document, wireless propagation in typical underground environments (e.g., mines and caverns with rough surfaces, curved galleries and side shafts) is a challenge to model theoretically with high precision and low complexity. As such, this field still presents many open research avenues. Available results at the state of the art provide "rules of thumb" and guidelines to understand the impact of various environmental characteristics (e.g., surface roughness) and to generate parameters for statistical simulations.

A significant number of theoretical analyses and experiments have been conducted on radio channel characteristics in tunnels. References [1]–[6] represent a sample of such studies generally carried out in tunnels with smooth surfaces, relatively large widths (e.g., large enough for trains or cars), and with at most mild curvatures. However, the open literature available on underground mining environments with rough surfaces, narrow widths, curves and side galleries is far more sparse [7]–[12]. Furthermore, as most previous mining environment propagation studies have dealt strictly with narrowband characteristics, this study is one of a few that has examined wideband statistical modeling (and particularly the impulse response structure) for these environments. Deterministic modeling is an alternative approach, e.g., the cascade impedance method [13] can be used on the basis that rough surface tunnels can be considered as a cascade of dielectric impedances with losses. This technique yields a significant complexity improvement with respect to previous deterministic approaches, but still requires a detailed segmented mapping and characterization of the environment. As such, in addition to providing new wideband measurement results at 2.4 GHz and 5.8 GHz, this work focuses on statistical modeling of the impulse response structure in confined environments with rough surfaces (such as underground mines) which, to the authors' knowledge, has not been addressed in the open literature.

A. Narrowband Radio Propagation Studies

The first comprehensive theoretical study of propagation characteristics in underground mines was performed in 1975 by Emslie *et al.* [7]. This work compared theoretical results with published measurements in coal mine tunnels, with a particular focus on the rate of loss of signal strength along a tunnel, and from one tunnel to another around a corner at frequencies in the range of 200–4000 MHz. The work modeled a straight section of the tunnel as a dielectric waveguide with rough surfaces and derived expressions relating the attenuation of radio waves in terms of wave polarization, radio frequency and tunnel dimensions. From this work, it was noted that the loss due to surface roughness increases with wavelength. Hence, while Emslie *et al.* mentioned that loss introduced by roughness is most important at low frequencies, loss introduced by tilt of the tunnel walls was shown to be most important at high frequencies. This theoretical work is highly rigorous, but using it to quickly predict propagation behavior in various

Manuscript received March 15, 2007; revised September 17, 2007. This work was presented in part at the IEEE Vehicular Technology Conference, Los Angeles, CA, September 26–29, 2004 and the IEEE Vehicular Technology Conference, Stockholm, Sweden, May 30–June 1, 2005.

M. Boutin and A. Benzakour are with the INRS-EMT, Université du Québec, Montreal, QC H2X 2C6, Canada and also with the LRCS-UQAT, Val d'Or, Montreal, QC J9P 1S2 Canada (e-mail: mathieu.boutin@emt.inrs.ca).

C. L. Despins and S. Affes are with the Partnerships for Research on Microelectronics, Photonics and Telecommunications (PROMPT)-Quebec, Montreal, QC H3A 2R7, Canada and also with the INRS-EMT, Université du Québec, Montreal, QC H2X 2C6, Canada.

Color versions of one or more of the figures in this paper are available online at http://ieeexplore.ieee.org.

Digital Object Identifier 10.1109/TAP.2007.913144

underground environments can be complex in view of the large number of site-specific parameters involved and in view of various simplifying assumptions.

Zhang [8] conducted experiments in two underground coal mines at 900 MHz on horizontal and vertical polarization. He observed that the propagation characteristics are quite different in the arched tunnels reinforced with concrete "passageways" (4.0–4.2 m wide and 3.0–3.5 m high) and in the "mining areas" which are rather irregular in shape and with no reinforcement. In the passageways, he noted that propagation exhibits guided wave characteristics in the region after a so-called "breakpoint" whose position is based on a hybrid tunnel propagation model consisting of a free space propagation zone on the near side of this breakpoint and of a modified waveguide propagation zone (with reduced attenuation) following the breakpoint. Zhang noted in [1] that the formula to calculate the location of the breakpoint in [14], [15] for urban microcells is inapplicable for tunnel microcells, and he proposed an equation for propagation along a LOS (line-of-sight) in tunnels which he applied to the "passageways" in the coal mines under study. He compared his results with data measured in various tunnels at different frequencies (900 MHz, 1.8 GHz and 2.448 GHz) and showed that the breakpoint depends strongly upon frequency, antenna position, and tunnel transversal dimensions. Zhang also indicated in [8] that no analogous theoretical model is available for the "mining areas" but that the waveguide model could provide somewhat approximate attenuation values, albeit while typically underestimating them.

Experiments made in CANMET at a 40 m depth [9], [10] have shown that the gallery curvature, passing from a LOS to a non-line-of-sight (NLOS) between transmitter and receiver antennas, has created two distinct areas of propagation, at both frequencies of 2.45 and 18 GHz [9]. At first glance, these results could be interpreted in terms of a hybrid propagation model. However, the value of w^2/λ is at this gallery, in the range of 200 m at 2.45 GHz and 1500 m at 18 GHz. As such, no waveguide effects are likely present in this case. It can be determined that the presence of these two areas of propagation is induced by the absence or presence of a LOS between the transmitter and the receiver [9], [10]. Other experiments in the same gallery at the same frequencies, but with additional people movement, have shown the signal envelope to follow a Rice distribution in the LOS case. For the NLOS case, the signal envelope still follows a Rice distribution, but changes to a Rayleigh distribution after several meters of distance between the two antennas.

B. Wideband Radio Propagation Characteristics

As indicated previously, the open literature available on wideband characteristics for underground mines is very limited and one usually resorts to results from more conventional tunnels as an approximation. As an example, Zhang reported [2], [4] at 900 MHz and 1.8 GHz, that the rms delay spread is generally less than 25 ns for a straight empty subway tunnel (3.34 m wide, 2.6 m high, 258.7 m long with rectangular cross sections) and increases to 103 ns in a tunnel occupied by vehicles. He also noted that higher frequencies tend to cause larger delay spreads. Liénard *et al.* [16] have observed rms delay spreads of 19 ns in LOS conditions in their underground mine gallery and of 25 ns to 42 ns in NLOS conditions. Hamalainen *et al.* [17] have observed that the total delay spread did not exceed 500 ns. Hamalainen's work is one of the few available studies on underground mine impulse response structure, albeit brief. They typically observed three dominant propagation paths with the first path always dominant and in 50% of observations, 16 dB higher than the second strongest path.

Fig. 1. Gallery at a 70 m depth.

Experiments made in CANMET at a 40 m depth and at a frequency of 2.4 GHz, in a gallery presenting a LOS and a NLOS areas between transmit-receive antennas, have shown an abrupt fall in receive power after a gallery curvature [10]. On the other hand, for a transmitter and a receiver located on opposite sides of the point of curvature of the gallery, the rms delay spread τ_{rms} has a relatively small value compared to the cases where the transmitter is closer to the receiver. This is probably due to the high path loss of the channel, which eliminates multipath components arriving with longer delays and reduces the number of detectable paths, implying a decrease of the τ_{rms} value.

II. Experimental Protocols

A gallery in CANMET, at a 70 m depth as depicted in Fig. 1, was used for these experiments at 2.4 and 5.8 GHz. This gallery has very rough surfaces, adjacent galleries, LOS and NLOS areas, and is very humid. The floor is flatter than the ceiling and the walls, and has some water puddles. The gallery stretches over a length of 70 m with a width of 2.5 to 3 m and is approximately 3 m in height. The CANMET gallery at a 40 m depth, in which the previous wideband measurements at 2.4 GHz were performed [10], was quite different than the one at a 70 m depth, as it was characterized by a width and height of both approximately 5 m.

The experimental protocol used to perform measurements in this gallery is based on measurements with omnidirectional antennas. A VNA (vector network analyzer) was used for transmission and reception of the radio frequency signal. Wideband measurements at 2.4 and 5.8 GHz were taken in the gallery with identical protocols at both frequencies. A bandwidth of 200 MHz has been used with a 1 MHz sweep frequency. The VNA has a minimal permitted sweep time of 75 ms for the considered bandwidth. With this value, a quasi-stationary state of

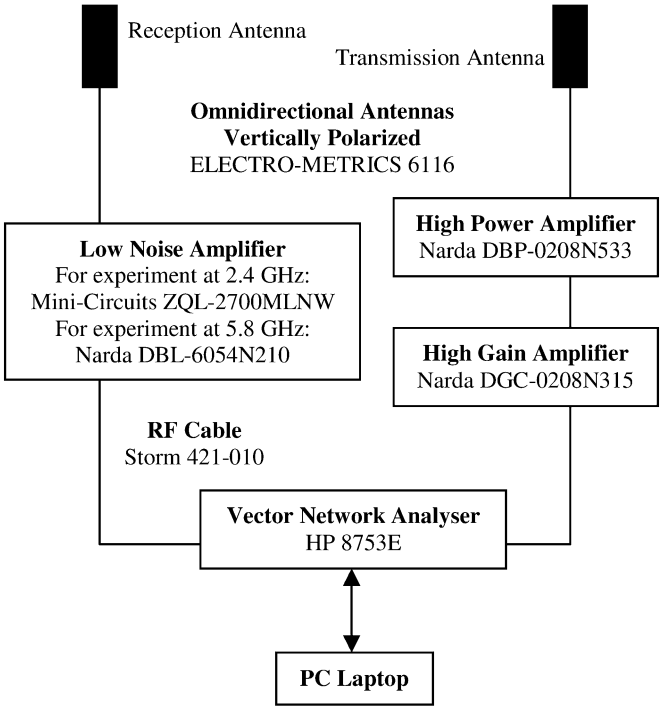

Fig. 2. Schematic diagram of the wideband measurement system.

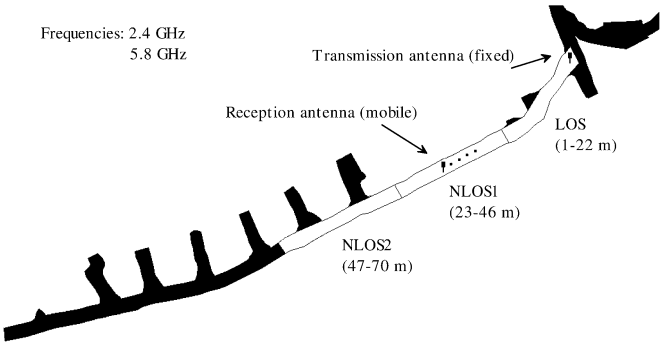

Fig. 3. Wideband experiments (only areas in white are considered).

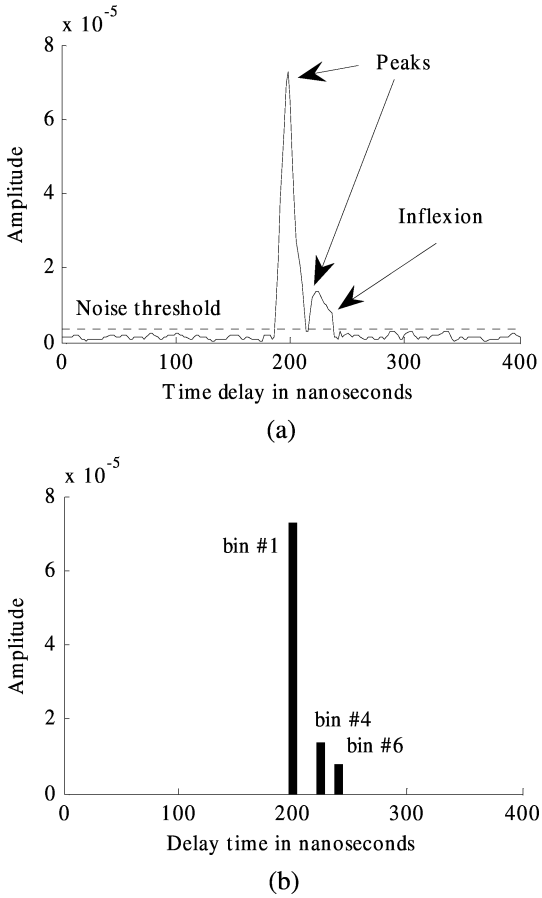

Fig. 4. Impulse response processing: (a) path identification and (b) time axis quantization.

the channel has been assumed during the measurements. Each sweep was composed of 201 samples spaced by 1 MHz. Prior to performing the measurements, the system was calibrated in order to filter the effect of the system frequency response.

To investigate the statistical behavior of the channel, experiments were conducted in which channel impulse response structures in the two bands of interest were compared for 420 different receiver locations along the gallery. The transmitter remained fixed and both transmitter and receiver antennas had a height of 1.8 m. The equipment used is shown in Fig. 2. For both frequencies, the transmit power was set to 10 dBm, the system noise floor was -140 dBm and the system dynamic range was 100 dBm.

Three separate areas of the mine gallery are considered—a LOS area and two NLOS areas (NLOS1 and NLOS2) of about 24 m in length—each depicted in Fig. 3. Hence, approximately 140 measurements were taken in each area, for each frequency.

The complex transfer function was obtained at all 420 measurement locations for each frequency. For each location, a temporal average has been performed on a set of ten measurements corresponding to different observation times. The time domain magnitude of the complex impulse response has been obtained from the measured samples of the frequency domain response, using the inverse Fourier transform (IFT). Considering the bandwidth of 200 MHz, the original time resolution was 5 ns (corresponding to the inverse of the bandwidth). In order to counter the effect of the 200 MHz windowing in an actual infinite bandwidth, the transfer functions are processed by a Hanning filter, thus lowering the time resolution to 8 ns. The time axis of each experimental impulse response is therefore quantized into bins of 8 ns duration, by considering the inflexions and peaks, to find the multiple paths of each impulse response [18]. The 1 MHz sweep frequency gives a temporal range of 1 μs (corresponding to the inverse of the sweep frequency), which is quite sufficient when compared to the highest maximum excess delay observed through all sets of measurements. Moreover, the noise is removed using a predefined threshold set to four times the standard deviation plus the mean of the noise measured over the tail of the considered impulse response. This threshold does not correspond to the system noise floor; it was determined empirically following a visual inspection of the set of all impulse responses. However, this definition may not be the same for different measurement hardware as the noise may then have a different magnitude. An example of such processing for each impulse response is depicted in Fig 4.

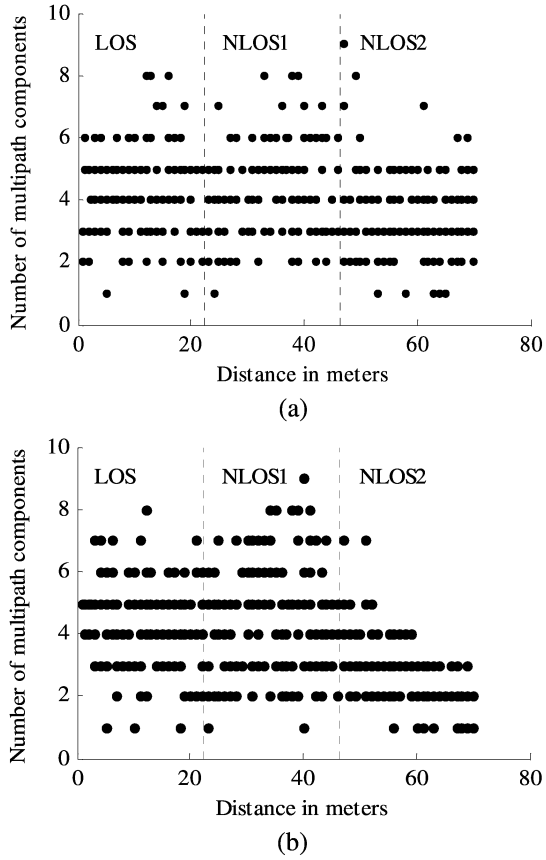

Fig. 5. Number of multipath components N as a function of distance at: (a) 2.4 GHz and (b) 5.8 GHz.

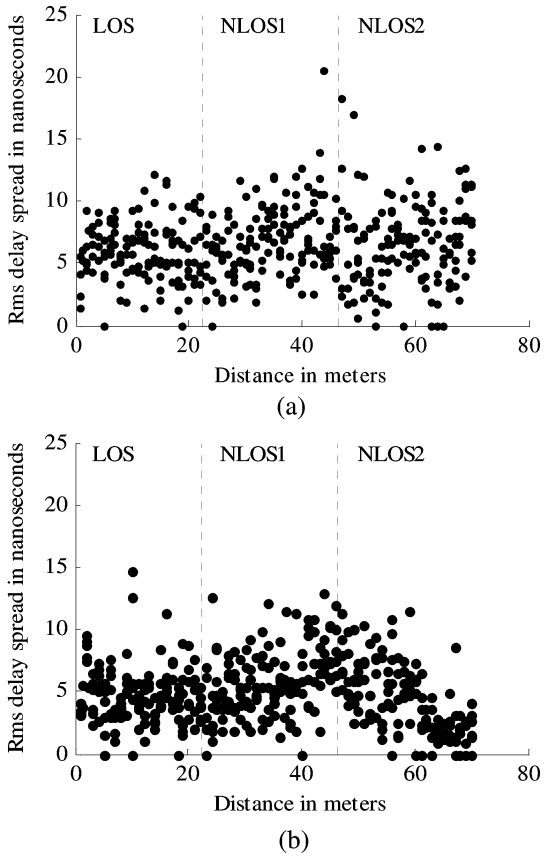

Fig. 6. Rms delay spread τ_{rms} as a function of distance at: (a) 2.4 GHz and (b) 5.8 GHz.

III. Measurement Results

The measurement results describe the time dispersion characteristics of the impulse responses, as well as the received power characteristics, for all 420 measurement locations and in both bands of interest.

A. Time Dispersion Characteristics

Figs. 5 and 6 illustrate the number of multipath components N and the rms delay spread τ_{rms}, as a function of the transmit-receive antenna separation for both frequencies.

These results show that, for the underground gallery considered and in the two frequency bands, random reflections have the effect of flattering the relationship between the rms delay spread and distance. Results were slightly different at the 40 m depth of the mine [10], where the gallery is wider (5 m in width), i.e., the rms delay spread exhibited little or no correlation with distance except at a specific breakpoint corresponding to the presence of a side shaft in the mine. As such, in both the 40 m depth and 70 m depth cases, the rms delay spread behavior as a function of distance in the mining environment differs from the correlation with distance which is frequently observed in indoor building environments with smooth surfaces. In fact, in [19], measurements at 10 GHz in office corridors showed that the rms delay spread follows a dual slope relation with a maximization point dependent on antenna directivity. Similarly, results in [20] at 950 MHz also showed that the rms delay spread has a peaked characteristic with respect to distance in empty indoor environments (meeting hall or shopping mall) and that the peak varies according to building dimensions and to the electrical properties of walls and windows. In indoor corridors but at much higher frequencies (i.e., 63 GHz) [21], the rms delay spread was again found to increase with transmitter-receiver separation up to a certain distance and to then decrease at larger separations. More recent results [22] at 2.11 GHz in different types of corridors and rooms also show, in a LOS corridor, an increase of rms delay spread with respect to distance followed by a decrease; however, the relationship between rms delay spread and distance was found to be less significant than with respect to path loss. In another study [23] at 60 GHz in a LOS corridor, the correlation between rms delay spread and distance was observed to be much smaller but to still exhibit a generally increasing and then decreasing trend beyond a certain distance. In [24], for the 2–6 GHz range, the rms delay spread was found to increase with distance while in the 900–1100 MHz and the 1.5–1.7 GHz bands in LOS office environments, the rms delay spread was found [25] to increase up to a certain distance and to then fluctuate around some mean value. Our results therefore tend to show that the correlation of the rms delay spread with respect to distance is far less likely in underground mines than in conventional indoor environments. This is likely due [10] to the scattering on the rough sidewalls' surface of the mines which can exhibit a difference of 25 cm between the maximum and minimum surface variations. However, comparisons of results herein for a gallery with a 2.5

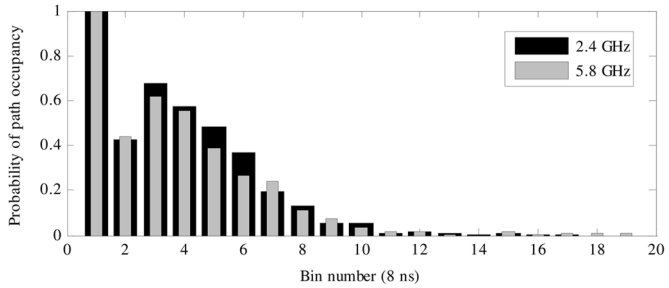

Fig. 7. Probability of path occupancy from the set of all impulse responses.

m width with those in [10] where the gallery has a 5 m width show that some correlation of rms delay spread with respect to distance seems to appear as the gallery becomes wider. It is also important to note that the rms delay spread values at each transmitter-receiver distance is based on an average of values obtained at different receiver positions between the two sidewalls. As such, results for a fixed receiver position with respect to the sidewalls could vary as the rms delay spread was also found [10] to be highly dependent on the bi-dimensional position of the receiver.

Fig. 7 illustrates the probability of path occupancy for each delay time bin of 8 ns. Fig. 8 shows the ratio of receiver positions for which the rms delay spread and the 90% coherence bandwidth are less than a specified value, i.e., the CDF (cumulative distribution function).

As the delay spreads were greater at 2.4 GHz in several locations (Fig. 6), the CDF plot for that band is consequently below the plot for the 5.8 GHz band in Fig. 8. It can be seen that, in the 2.4 GHz band, the rms delay spread is less than or equal to 6.34 ns for 50% of all locations. The corresponding value for the 5.8 GHz band is 4.98 ns. Furthermore, Fig. 7 shows that after 80 ns, the probability of having path arrivals is very small for both frequencies. This probability of path occupancy is quite different from what has been observed in another mine [17] at a center frequency of 1 GHz, where it is likely to have path arrivals up to 4.6 μs. The frequency band, as well as the different structural characteristics of this other mine, reinforce the point that underground mine propagation behavior can be highly site-specific.

For wideband radio systems in such an environment, performance levels under static conditions would thus be marginally better in the 5.8 GHz band (assuming multipath diversity is not exploited), since delay spreads are slightly smaller in this band than at 2.4 GHz as shown in Fig. 8(a). As such, and as can be seen in Fig. 8(b), the coherence bandwidth at 5.8 GHz tends to be wider than at 2.4 GHz, the latter frequency band imposing therefore a narrower frequency band for efficient communication (e.g., the need for a powerful equalizer would be more important). Consequently, we can say that the maximum usable data rate with a relatively simple transceiver would be higher at 5.8 GHz than at 2.4 GHz in this underground environment.

The mean, standard deviation and maximum of N (number of multipath components), τ_{m} (mean excess delay), τ_{rms} (rms delay spread) and $\tau_{\max}$ (maximum excess delay) in both bands have been computed from the time domain responses and are summarized in Table I.

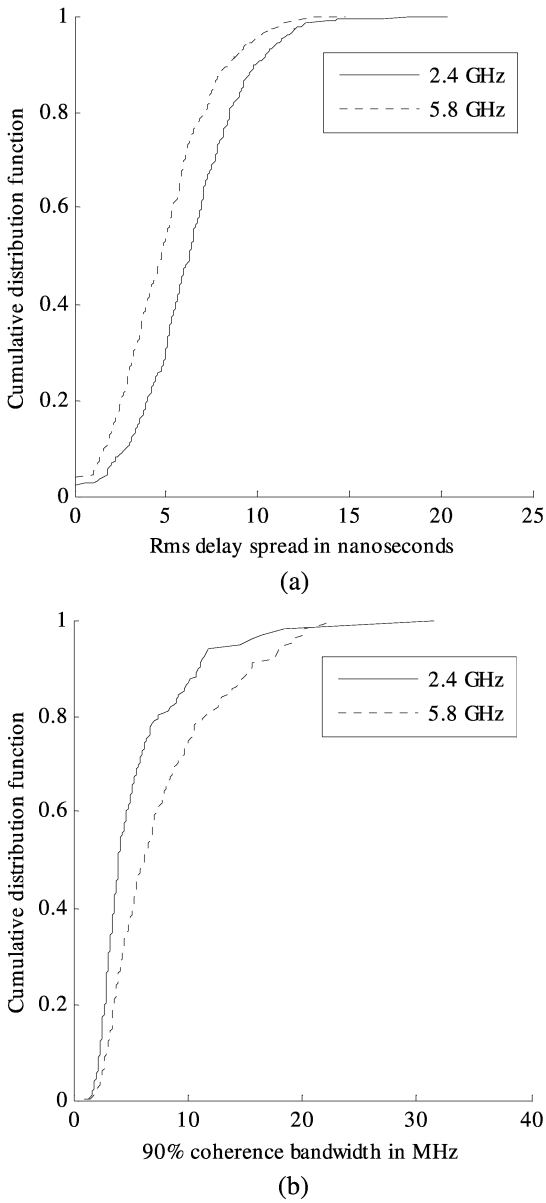

Fig. 8. Cumulative distribution function of: (a) rms delay spread and (b) 90% coherence bandwidth, at 2.4 and 5.8 GHz.

By comparing the results at 2.4 GHz with those obtained at the same frequency in another gallery at CANMET [10], we can see that $\tau_m, \tau_{\mathrm{rms}}$ and $\tau_{\max}$ have smaller values in our case, probably due to site-specific configuration. Indeed, the gallery studied in [10] is wider and has more important side galleries. Zhang *et al.* [2], [4], with center frequencies of 900 MHz and 1800 MHz, have obtained very short delay spreads as compared to our results for an empty straight tunnel [4], but they have obtained even greater delay spreads than our results when the tunnel was obstructed by a vehicle. They have obtained greater rms delay spread as compared to our results for five different tunnels (emptied and occupied conditions), some being straight, others being interconnected or curved [2]. Contrary to our results, measurements in [2], [4] for tunnels revealed that higher frequency caused larger rms delay spreads.

TABLE I
MEAN, STANDARD DEVIATION AND MAXIMUM OF N, T_M, T_{RMS} AND T_{MAX} AT 2.4 AND 5.8 GHZ

All locations	mean		std		max	
	2.4 GHz	**5.8 GHz**	**2.4 GHz**	**5.8 GHz**	**2.4 GHz**	**5.8 GHz**
N	4	3.9	1.5	1.8	9	9
τ_m (ns)	3.21	2.30	3.24	2.61	18.51	15.83
τ_{rms} (ns)	6.49	5.11	3.07	2.74	20.40	14.74
τ_{max} (ns)	42.38	46.23	30.76	45.62	232	240

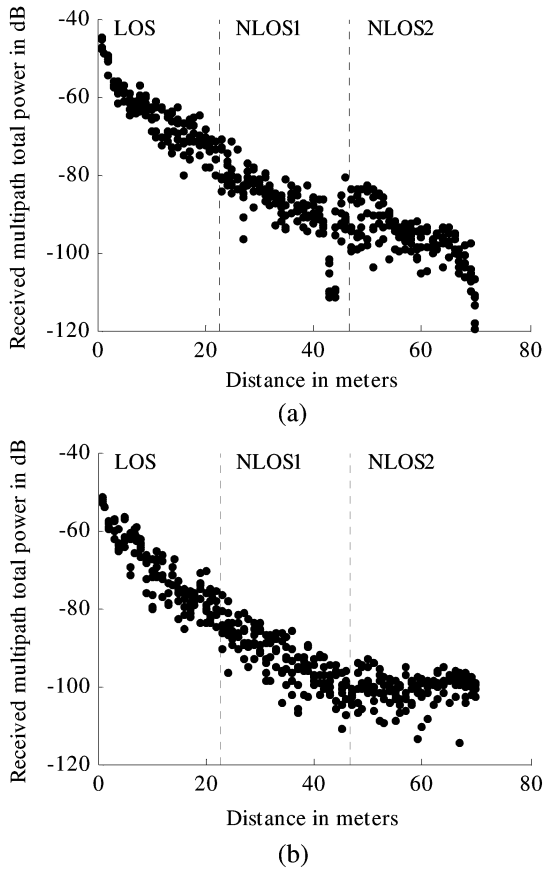

Fig. 9. Received multipath total power as function of distance at: (a) 2.4 GHz and (b) 5.8 GHz.

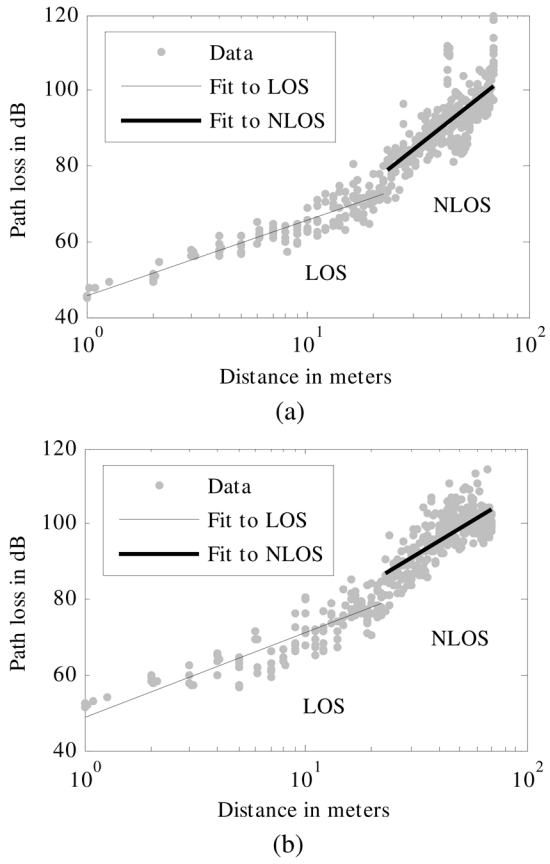

Fig. 10. Path loss as function of distance at: (a) at 2.4 GHz and (b) 5.8 GHz.

Wall roughness in our case may be the reason for that propagation difference as function of frequency. Our results demonstrate higher delay spreads in our mine gallery as compared to the mine studied by Liénard *et al.* [16] at lower frequencies, even in obstructed LOS conditions.

B. Received Power Parameters

Fig. 9 illustrates the received multipath total power P (relative to the transmitted power) versus distance, which is the power sum of all path arrivals for a given impulse response.

The results show that the curvature of the gallery located at about 17 m from the transmitter does not have a visible effect on the attenuation of the signal in both frequency bands, with the attenuation remaining close to the free space value on both sides of the curvature. Based on a hybrid propagation model interpretation (defined in [8] for rectilinear mine tunnels), this area would thus still be within the first Fresnel zone clearance as w^2/λ is, in this gallery of 3 m maximum width ($w = 3$ m), in the range of 75 m at 2.4 GHz ($\lambda = 0.122$ m) and 170 m at 5.8 GHz ($\lambda = 0.052$ m).

However, an abrupt fall in the power of the signal in the 2.4 GHz band was noticed for the two specific transmitter-receiver spacings of 43 and 44 m. The same phenomenon was noticed at approximately 70 m, still at 2.4 GHz. This can likely be explained by multipath destructive combinations resulting from local gallery topology. On the other hand, a slight increase in the multipath total power for some receiver locations, at both frequency bands, was recorded between 47 and 53 m. The number of multipath components varies marginally at these distances as shown in Fig. 5. This increase is probably a result of the variation in the phase of the paths induced by the first connecting gallery (this gallery is about 7 m deep), possibly implying constructive combinations. This is more visible in the 2.4 GHz band. It should be noted again that these local signal variations are likely highly site-specific (e.g., with the presence of connecting side galleries).

Path loss as function of distance is shown in Fig. 10 for both frequencies. The path loss values for the LOS and NLOS

TABLE II
MEAN PATH LOSS AT THE REFERENCE DISTANCE, PATH LOSS EXPONENT AND STANDARD DEVIATION OF THE RANDOM VARIABLE X

Frequency	Area	Mean path loss at d_0 (dB)	α	σ_X (dB)
2.4 GHz	LOS (d_0 = 1 m)	45.40	2.03	3.09
	NLOS (d_0 = 23 m)	78.80	4.62	5.39
5.8 GHz	LOS	48.97	2.22	4.05
	NLOS	86.90	3.51	4.52

(NLOS1 and NLOS2 together) areas are evaluated separately. The received multipath total power in these areas is likely to fluctuate differently, even if that difference is not obvious in Fig. 9. Path loss in the channel is normally distributed in decibels (dB) with a linearly increasing mean and is modeled as

$$\mathrm{PL}_{\mathrm{dB}}(d) = \overline{\mathrm{PL}}_{\mathrm{dB}}(d_0) + 10\alpha \log\left(\frac{d}{d_0}\right) + X \qquad (1)$$

where $\overline{\mathrm{PL}}_{\mathrm{dB}}(d_0)$ is the mean path loss at the reference distance d_0, $10\alpha\log(d/d_0)$ is the mean path loss referenced to d_0, and X is a zero mean Gaussian random variable expressed in dB. The mean path loss at d_0 and the path loss exponent α were determined through least square regression analysis [24]. The difference between this fit and the measured data is represented by the Gaussian random variable X. Table II lists the values obtained for $\overline{\mathrm{PL}}_{\mathrm{dB}}(d_0)$, α, and σ_X (standard deviation of X).

Fig. 10 and Table II show that there is no significant difference regarding path loss at 2.4 and 5.8 GHz in this mine gallery. In both cases, by considering all the measurements from 1 m to 70 m, coverage would be relatively similar, albeit slightly better at 2.4 GHz. For the LOS area, the 2.4 GHz band yields a propagation exponent very close to free space (where $\alpha = 2$), while the exponent is larger in the 5.8 GHz band, in addition to a greater path loss fluctuation and a greater mean path loss at d_0. For the NLOS area however, the path loss exponent is smaller at 5.8 GHz than at 2.4 GHz with, in addition, a smaller path loss fluctuation; however the mean path loss at d_0 does remain higher (as expected at a higher frequency).

From measurements at 2.4 GHz in another gallery at CANMET [10], the path loss exponent was around 2.2 over the entire length of the gallery for both LOS and NLOS situations as well as with the impact of adjacent galleries. This result is comparable to our LOS situation at the same frequency, although we have obtained a smaller value. However, our NLOS situation gives a much greater path loss exponent. The difference in gallery dimensions and configurations play an important role in these results. In [17], propagation measurements in a mine tunnel resulted in a path loss exponent of 4.0 in a straight cave and 8.0 in a curved one. Although they have used a smaller frequency (1 GHz) this represents roughly twice the values we have obtained. The particularity of this environment (LOS and NLOS situations with many side galleries) may explain this great difference with our results. Zhang *et al.* [2], [4], at frequencies of 900 and 1800 MHz, found out that propagation loss is higher in curved or branched tunnels than in straight tunnels. This is in concordance with our results (LOS compared to NLOS). In [2], they have obtained slightly higher path loss exponents and standard deviations, as compared to our results. Because their five different tunnels may be emptied, occupied, straight, interconnected or curved, it may have an impact on radio wave propagation and degrade received signal power more than in our mine gallery. Finally, path loss seems to be more severe in our mine than the one studied by Liénard *et al.* [16], perhaps as a result of higher frequencies used in our case and because of the different mine environments.

IV. WIDEBAND STATISTICAL MODELING

As propagation characteristics specific to such confined environments with rough surfaces have been observed, a deterministic approach to wideband modeling was developed [13] as an initial step. However, this approach can be very complex in capturing the very specific nature of propagation in a confined gallery with rough surfaces. Its results are also highly site-specific and dependent upon a large number of environmental parameters.

This section thus reports on the results of a wideband statistical modeling approach for channel characterization in underground mines. Statistical modeling is attractive in that it can quickly and reliably generate simulated impulse responses for a particular frequency and topography based on accurate models derived from experimental measurements. As opposed to the time-consuming process of gathering a huge amount of experimental impulse responses, simulated impulse responses can be readily available to test new applications for mines such as wireless geolocation [26].

Prior to beginning the modeling process, the path loss, which is superfluous in this specific part of the modeling process, was removed prior to testing the candidate amplitude distribution with the experimental impulse responses. However, the path loss is reinserted during the simulation process in order to reflect the real propagation environment.

A radio propagation channel can be completely characterized by its random impulse response $h(t)$ as per

$$h(t) = \sum_{k=0}^{N-1} a_k \delta(t - t_k) e^{j\theta_k} \qquad (2)$$

where N is the number of multipath components, α_k, t_k and θ_k are the random amplitude, arrival-time and phase of the kth path, respectively, and δ is the delta function. The path arrivals t_k and amplitudes α_k are modeled in the following sections by comparing them to some already known distributions frequently used in the literature. The phases θ_k are assumed to be, a priori, statically independent uniform random variables distributed over $[0, 2\pi)$.

A. Path Arrival Modeling

The modeling process considers the following distributions for path arrivals, which are the most commonly used in the literature [27]: Poisson, modified Poisson, and Weibull. The comparison is based upon the probability of having a certain number of path occurrences since the second time bin, up to the set of all

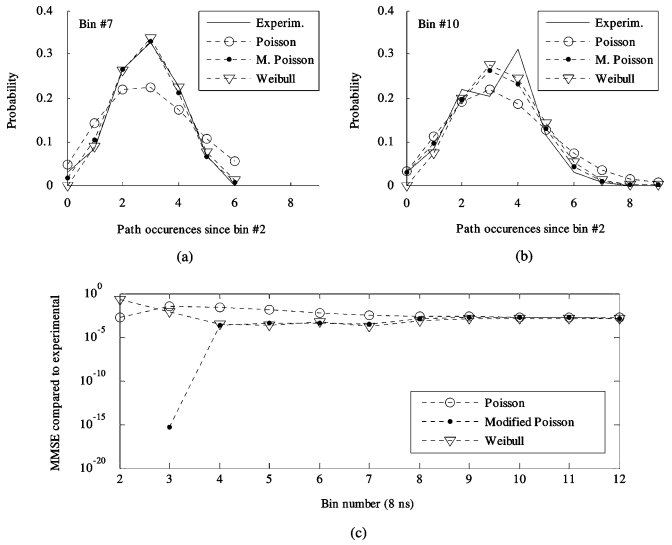

Fig. 11. Example of distributions comparison for the number of impulses up to a fixed time bin number (2.4 GHz, LOS). (a) Probability of path occurrences from bin #2 up to bin #7, (b) probability of path occurrences from bin #2 up to bin #10, (c) MMSE obtained from all three distributions compared to experimental results, for all bin numbers.

time bins. The first time bin is not considered because path occurrence for that bin is deterministic (always present). As an example, Fig. 11(a) and (b) shows the distribution for the number of path occurrences for the 7th and 10th time bin, respectively, but a similar distribution is actually obtained for all time bins. The parameters of each of these distributions are estimated from experimental measurements, based on minimum mean square error (MMSE), and results suggest that the modified Poisson distribution offers the best fit for all areas and both frequencies, as shown in Fig. 11(c).

In 1987, Saleh *et al.* [28] added an alternative to the conventional Poisson model after observing that impulses arrive in clusters in typical indoor environments such as offices. Each cluster occurs with a certain arrival rate, and each impulse occurs with another arrival rate within each cluster. Since we have not observed any clustering effect in our impulse responses, clustering has not been included in our modeling process. This is likely as a result of the highly random reflection and diffraction effects caused by the rough wall surfaces of these mine gallery environments. However, the Modified Poisson distribution, because of its high flexibility, can be used to model this specific multipath randomness.

B. Path Amplitude Modeling

The most popular distributions for path amplitude, especially for indoor environments, are considered as candidate models [27]: Rayleigh, Rice, Nakagami, Weibull, and lognormal. In order to estimate the parameters of each candidate distribution at each time bin, the method of moments is used with the experimental results [29]. A curve-fitting technique is used to obtain decreasing exponential curves of the form

$$y = Ae^{-(x-1)/B} + C \tag{3}$$

for both amplitude average and standard deviation as a function of time bins, as depicted by the example of Fig. 12. The first and second fitted moments can be used to approximate the parameters of the five amplitude distributions for each bin, with

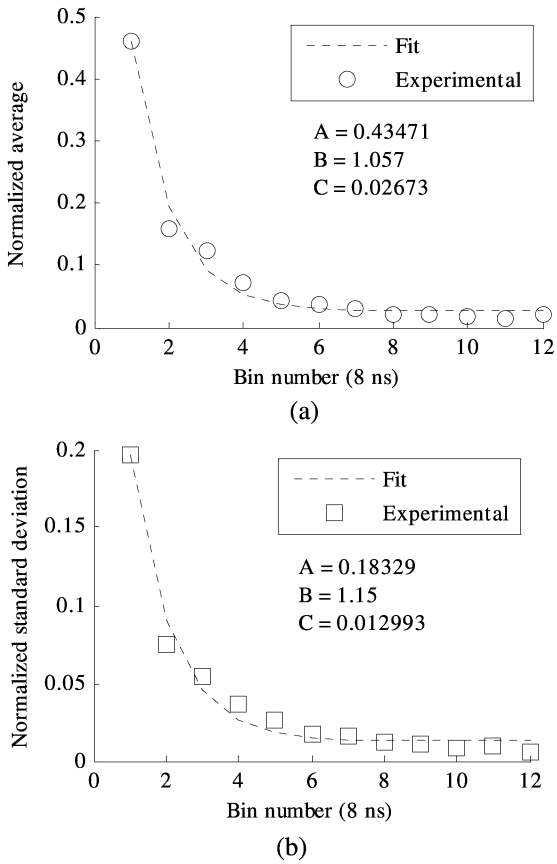

Fig. 12. Example of both normalized amplitude: (a) average and (b) standard deviation exponential curves (2.4 GHz, LOS).

these two statistical properties. The simulation process is however required to determine which of these distributions is the most appropriate to model the channel.

C. Simulation Process

Three steps are needed in order to simulate impulse responses. First, a set of path arrivals (including all the time bins) is generated following the Modified Poisson distribution with its optimal parameters for each bin found during modeling. Second, five sets of path amplitudes are generated following the Rayleigh, Rice, Nakagami, Weibull, and lognormal distributions, with their optimal parameters for each bin found during modeling. Finally, each of the generated sets of path arrivals is combined with the sets of path amplitude, resulting in a simulated impulse response. One could also reinsert the path loss effect that has been removed prior to path amplitude modeling.

As the rms delay spread is the main comparison criterion, it is extracted from both simulated and experimental impulse responses. The Kolmogorov–Smirnov test is then used to identify the distribution which best represents the experimental results, based on this most commonly used propagation characteristic. An example of this test is presented in Fig. 13.

After comparing a set of 100 simulations to the experimental results, each simulation including 3000 impulse responses, the best amplitude distribution for each area of the mine tunnel and for each frequency is shown in Table III, where the performance score of each distribution is reported. The results shown in Table III clearly suggest that the best amplitude distribution,

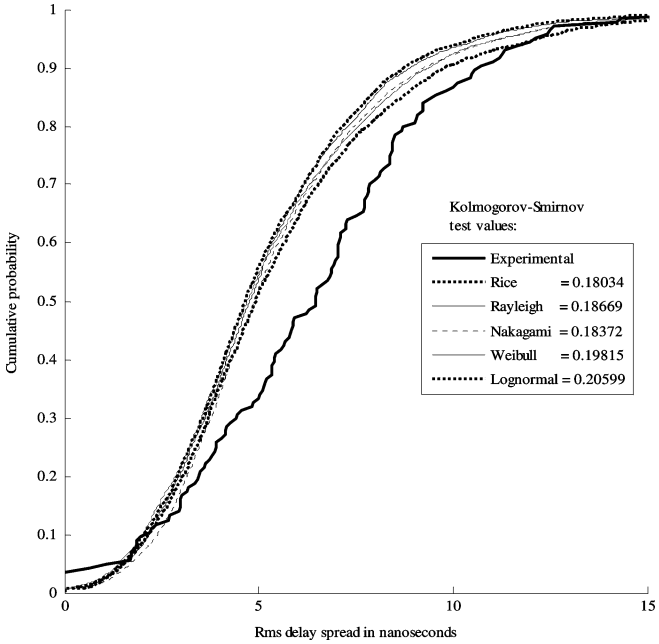

Fig. 13. Example of the Kolmogorov–Smirnov test for the rms delay spread (2.4 GHz, LOS).

TABLE III
SIMULATIONS MATCH RESULTS IN % BASED ON THE RMS DELAY SPREAD

	LOS	NLOS1	NLOS2
2.4 GHz:			
Rayleigh	0	88	92
Rice	91	0	0
Nakagami	2	4	2
Weibull	7	6	5
Lognormal	0	2	1
5.8 GHz:			
Rayleigh	1	90	94
Rice	89	2	1
Nakagami	2	4	3
Weibull	8	2	1
Lognormal	0	2	1

regardless of frequency, is Rice for a LOS propagation, and Rayleigh for a NLOS situation. The best distribution for path arrivals is the Modified Poisson, as mentioned previously.

The most relevant models could provide simulations that could be used in many upcoming projects that need a large impulse response data base representing the studied mine tunnel. Further work will seek to compare results of this statistical modeling approach with those of deterministic modeling.

V. CONCLUSION

This paper has focused on empirical and statistical approaches to describe the path loss effects and impulse response structure. This approach lends itself naturally to the use of channel simulators and emulators. There is relatively little propagation measurement data openly available for underground environments. It then makes it all the more important to understand, at least in terms of trends, the impact of various environmental characteristics when providing parameters for statistical simulations.

This work is one of only a few that has provided openly available results dealing with impulse response structure in these underground environments. This structure was found to differ from the one observed in more conventional indoor environment (e.g., offices and corridors) in two respects. First, while path arrivals in office environments are often characterized by clusters, no such phenomenon was observed in the mine galleries and the path arrival process can be described by a single statistical distribution. Second, while rms delay spread against distance in indoor corridor environments frequently exhibits correlation with respect to distance, rms delay spread shows very little correlation with distance in the mine galleries, particularly when the gallery is narrow. Both these observations are likely the result of the rough wall surfaces which highly randomize the multipath phenomena.

The measurement results have shown that delay spread is more severe at 2.4 GHz than at 5.8 GHz in this underground environment, but the coverage is somewhat superior at 2.4 GHz. A higher data rate could thus be supported when deploying a relatively simple transceiver (i.e., without exploiting multipath diversity) using the 5.8 GHz frequency band, as it offers a wider coherence bandwidth. Results also show that the NLOS area will only yield a weaker received signal as compared to the LOS area, with approximately the same delay spread. Thus, with sufficient transmitted power, the deployment of WLAN access points would not necessarily need to be done on a LOS basis, therefore limiting the overall system cost.

It is clear that wireless propagation in underground mine tunnels can be a challenge to model accurately in view of the complexity of the environment. As such, further narrowband and wideband measurement campaigns should be also undertaken in galleries with different configurations and at different operating frequencies.

REFERENCES

[1] Y. P. Zhang, "Novel model for propagation loss prediction in tunnels," *IEEE Trans. Veh. Technol.*, vol. 52, no. 5, pp. 1308–1314, Sep. 2003.
[2] Y. P. Zhang and Y. Hwang, "Characterization of UHF radio propagation channels in tunnel environments for microcellular and personal communications," *IEEE Trans. Veh. Technol.*, vol. 47, no. 1, pp. 283–296, Feb. 1998.
[3] T. Klemenschits and E. Bonek, "Radio coverage of road tunnels at 900 and 1800 MHz by discrete antennas," in *Proc. 5th IEEE Int. Symp. on Personal, Indoor and Mobile Radio Communications (PIMRC 1994)*, Sep. 1994, pp. 411–415.
[4] Y. P. Zhang, Y. Hwang, and R. G. Kouyoumjian, "Ray-optical prediction of radio-wave propagation characteristics in tunnel environments—Part 2: Analysis and measurements," *IEEE Trans. Antennas Propag.*, vol. 46, no. 9, pp. 1337–1345, Sep. 1998.
[5] F. M. Pallarés *et al.*, "Analysis of path loss and delay spread at 900 MHz and 2.1 GHz while entering tunnels," *IEEE Trans. Veh. Technol.*, vol. 50, no. 3, pp. 767–776, May 2001.
[6] Y. P. Zhang *et al.*, "Measurements of the propagation of UHF radio waves on an underground railway train," *IEEE Trans. Veh. Technol.*, vol. 49, no. 4, pp. 1342–1347, Jul. 2000.
[7] A. Emslie, R. Lagace, and P. Strong, "Theory of the propagation of UHF radio waves in coal mine tunnels," *IEEE Trans. Antennas Propag.*, vol. 23, no. 2, pp. 192–205, Mar. 1975.
[8] Y. P. Zhang, G. X. Zheng, and J. H. Sheng, "Radio propagation at 900 MHz in underground coal mines," *IEEE Trans. Antennas Propag.*, vol. 49, no. 5, pp. 757–762, May 2001.
[9] M. Djadel, C. Despins, and S. Affes, "Narrowband propagation characteristics at 2.45 and 18 GHz in underground mining environments," in *Proc. IEEE GLOBECOM 2002*, Taipei, Taiwan, Nov. 2002, vol. 2, pp. 1870–1874.

[10] C. Nerguizian, C. Despins, S. Affes, and M. Djadel, "Radio channel characterization of an underground mine at 2.4 GHz," *IEEE Trans. Wireless Commun.*, vol. 4, no. 5, pp. 2441–2453, Sep. 2005.
[11] G. X. Zheng, J. H. Sheng, and Y. P. Zhang, "Propagation of UHF radio waves in trapezoidal tunnels," *Microw. Opt. Technol. Lett.*, vol. 20, pp. 295–297, Jan. 1999.
[12] Y. P. Zhang, T. S. Ng, G. X. Zheng, J. H. Sheng, and Y. Q. Wang, "Radio propagation within coal mine long wall faces at 900 MHz," *Microw. Opt. Technol. Lett.*, vol. 18, pp. 184–187, Jul. 1998.
[13] M. Ndoh and G. Y. Delisle, "Underground mines wireless propagation modelling," presented at the IEEE VTC'04-Fall, Los Angeles, CA, Sep. 26–29, 2004.
[14] H. H. Xia *et al.*, "Radio propagation characteristics for line-of-sight microcellular and personal communications," *IEEE Trans. Antennas Propag.*, vol. 41, no. 10, pp. 1439–1447, Oct. 1993.
[15] M. J. Feuertein *et al.*, "Path loss, delay spread, and outage models as function of antenna height for microcellular system design," *IEEE Trans. Veh. Technol.*, vol. 43, pp. 487–497, Aug. 1994.
[16] M. Liénard and P. Degauque, "Natural wave propagation in mine environments," *IEEE Trans. Antennas Propag.*, vol. 48, no. 9, pp. 1326–1339, Sep. 2000.
[17] M. Hamalainen, J. Talvitie, V. Hovinen, and P. Leppanen, "Wideband radio channel measurement in a mine," in *Proc. 5th Int. Symp. on Spread Spectrum Techniques and Applications (ISSSTA 98)*, Sun City, South Africa, Sep. 1998, vol. 2, pp. 522–526.
[18] G. L. Turin, F. D. Clapp, T. L. Johnston, S. B. Fine, and D. Lavry, "A statistical model of urban multipath propagation," *IEEE Trans. Veh. Technol.*, vol. 21, no. 1, Feb. 1972.
[19] A. F. AbouRaddy, S. M. Elnoubi, and A. El-Shafei, "Wideband measurements and modeling of the indoor radio channel at 10 GHz, Parts I and II," presented at the 15th National Radio Science Conf., Cairo, Egypt, Feb. 24–26, 1998.
[20] R. J. C. Bultitude *et al.*, "The dependence of indoor radio channel multipath characteristics on transmit/receive ranges," *IEEE J. Select. Areas Commun.*, vol. 11, no. 7, pp. 979–990, Sep. 1993.
[21] A. Hammoudeh and D. A. Scammell, "Frequency domain characterization of LoS nonfading indoor wireless LAN channel employing frequency and polarization diversity in the 63.4–65.4 GHz band," *IEEE Trans. Veh. Technol.*, vol. 53, no. 4, pp. 1176–1189, Jul. 2004.
[22] S. Salous and V. Hinostroza, "Wideband indoor frequency agile channel sounder and measurements," *Proc. Inst. Elect. Eng. Microwaves, Antennas and Propagation*, vol. 152, no. 6, pp. 573–580, Dec. 2005.
[23] S. Geng, J. Kivinen, and P. Vainikainen, "Propagation characterization of wideband indoor radio channels at 60 GHz," in *Proc. IEEE Int. Symp. on Microwave, Antenna, Propagation and EMC Technologies for Wireless Communications*, Aug. 2005, vol. 1, pp. 314–317.
[24] J. A. Dabin, A. M. Haimovich, and H. Grebel, "A statistical ultra-wideband indoor channel model and the effects of antenna directivity on path loss and multipath propagation," *IEEE J. Select. Areas Commun.*, vol. 24, no. 4, pp. 752–758, Apr. 2006.
[25] H. Zaghloul, M. Fattouche, G. Morrison, and D. Tholl, "Comparison of indoor propagation channel characteristics at different frequencies," *Electron. Lett.*, vol. 27, no. 22, pp. 2077–2079, Oct. 1991.
[26] C. Nerguizian, C. Despins, and S. Affes, "Geolocation in mines with an impulse response fingerprinting technique and neural networks," *IEEE Trans. Wireless Commun.*, vol. 5, no. 3, pp. 603–611, Mar. 2006.
[27] H. Hashemi, "The indoor radio propagation channel," *Proc. IEEE*, vol. 81, no. 7, pp. 943–968, Jul. 1993.
[28] A. Saleh and R. Valenzuela, "A statistical model for indoor multipath propagation," *IEEE J. Select. Areas Commun.*, vol. 5, no. 2, pp. 128–137, Feb. 1987.
[29] R. Ganesh and K. Pahlavan, "Statistical modelling and computer simulation of indoor radio channel," *Proc. Inst. Elect. Eng. Communications, Speech and Vision*, vol. 138, no. 3, pp. 153–161, Jun. 1991.

Mathieu Boutin received the Bachelor's degree in computer science engineering from the École Polytechnique de Montréal, Montreal, QC, Canada, in 2002, and the Master's degree from INRS-EMT, Université du Québec, Montreal, in 2005, where he is currently working toward the Ph.D. degree.

His research interests are in radio wave propagation and cognitive wireless *ad hoc* networks.

Ahmed Benzakour received the Bachelor's degree in physics science from Université Mohammed V, Rabat, Morocco, in 1997 and the Master's degree from INRS-EMT, Université du Québec, Montreal, Canada, in 2005.

Currently, he is with the INRS-EMT, Université du Québec and also with LRCS-UQAT, Montreal, QC, Canada. His research interests are in radio channel propagation characteristics and cooperative communications in cognitive wireless networks.

Charles L. Despins (S'93–M'94–SM'02) received the Bachelor's degree in electrical engineering from McGill University, Montréal, QC, Canada, in 1984, and the Master's and Ph.D. degrees from Carleton University, Ottawa, ON, Canada, in 1987 and 1991, respectively.

From 1992 to 1996, he was a Faculty Member of the Institut National de la Recherche Scientifique (INRS), Université du Québec, Montréal, Canada, following employment in 1984 to 1985 with CAE Electronics as a Member of the Technical Staff, and in 1991 to 1992 with the Department of Electrical and Computer Engineering, École Polytechnique de Montréal, Canada, as a Lecturer and a Research Engineer. From 1996 to 1998, he was with Microcell Telecommunications Inc., a Canadian GSM operator, and was responsible for industry standard and operator working groups, as well as for technology trials and technical support for joint venture deployments in China and India. From 1998 to 2003, he was Vice-President and Chief Technology Officer of Bell Nordiq Group Inc., a wireless and wireline network operator in northern and rural areas of Canada. Since 2003, he has been President and CEO of Partnerships for Research on Microelectronics, Photonics and Telecommunications (PROMPT)-Quebec, Montreal, a university-industry research consortium in the field of information and communications technologies. He remains an Adjunct Professor at INRS-EMT, Montreal, QC, Canada with research interests in wireless communications.

Dr. Despins is a Member of the Order of Engineers of Québec and is also a Fellow of the Engineering Institute of Canada. He was awarded the IEEE Vehicular Technology Society Best Paper of the Year prize in 1993 as well as the Outstanding Engineer Award in 2006 from IEEE Canada.

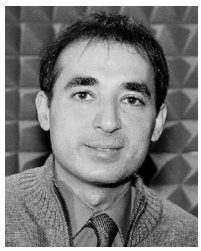

Sofiène Affes (S'94–M'95–SM'04) received the Diplôme d'Ingnieur in electrical engineering and the Ph.D. degree (with honors) in signal processing both from the École Nationale Supérieure des Télécommunications (ENST), Paris, France, in 1992 and 1995, respectively.

In 1995, he joined the INRS-EMT, University of Quebec, Montreal, QC, Canada, where he was a Research Associate from 1995 to 1997, an Assistant Professor from 1997 to 2000, and he is currently an Associate Professor in the Wireless Communications Group. His research interests are in wireless communications, statistical signal and array processing, adaptive space-time processing and MIMO. From 1998 to 2002, he lead the radio-design and signal processing activities of the Bell/Nortel/NSERC Industrial Research Chair in Personal Communications at INRS-EMT. Currently he is actively involved in a major project in wireless of PROMPT-Quebec (Partnerships for Research on Microelectronics, Photonics and Telecommunications).

Prof. Affes is the co-recipient of the 2002 Prize for Research Excellence of INRS and currently holds a Canada Research Chair in Wireless Communications. He served as a General Co-Chair of the IEEE VTC'2006-Fall conference, Montreal, Canada, and currently acts as a member of Editorial Board of the Wiley Journal on Wireless Communications and Mobile Computing.